Factors contributing to the summer 2003 European heatwave

Emily Black
Mike Blackburn
Giles Harrison
Brian Hoskins
John Methven

Department of Meteorology, University of Reading

European temperature record

Europe was exceptionally warm and dry from May through to the end of August 2003. Figure 1 shows the European average surface air temperature (at 2 m) derived from global analyses of the European Centre for Medium-Range Weather Forecasts (ECMWF). The analyses are calculated for every 6-hour period at 0000, 0600, 1200 and 1800 GMT. The daily average is also shown for comparison with the daily climatology for 1958–2002 obtained from the ECMWF re-analysis project (ERA-40, see Simmons and Gibson 2000). The heatwaves in June and early August can readily be identified. During these periods even the night-time temperatures exceeded the climatological mean daily temperatures! Averaging over each month the temperature anomalies were +4.2 degC in June, +3.8 degC in August and almost +2 degC in May and July. The temperature anomalies were most extreme in France and Switzerland although maximum temperature records were broken in many parts of Europe. For example, Schär *et al.* (2004) have shown that the June–July–August temperature averaged for four Swiss stations exceeded the 1864–2000 mean by 5.1 degC – far greater than the next highest anomaly of +2.7 degC in 1947. Both Beniston (2004) and Schär *et al.* (2004) argue that a repeat of the 2003 summer would be extremely unlikely if stationarity of climate statistics were to be assumed, but that the temperatures experienced across Europe in summer 2003 could be considered 'normal' by the end of the twenty-first century under a high greenhouse-gas emissions scenario. Given the increased human mortality experienced during the 2003 heatwave (World Health Organization (WHO) 2003; Kovats *et al.* 2004), this has important implications for future human health.

Here we attempt to draw together the factors that may have contributed to this exceptional summer by examining the large-scale atmospheric flow and the regional heat budget from ECMWF analyses and measurements of the surface energy budget at the University of Reading. The influence of atmospheric flow anomalies on the surface of the land and ocean, and possible feedbacks are also discussed.

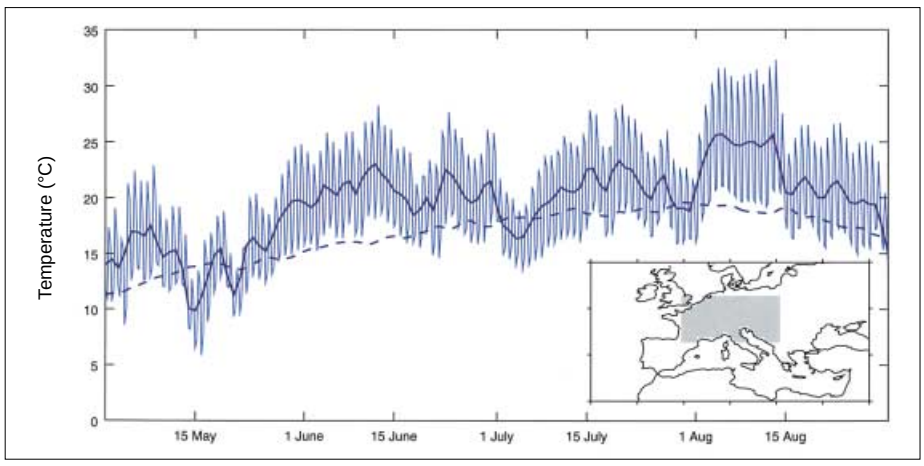

Fig. 1 Time-series of 2 m air temperature for summer 2003 from ECMWF operational analyses averaged over Europe (the land region shaded grey in the inset). The analyses were calculated for the regular times 0000, 0600, 1200, 1800 GMT, and the daily average is also shown (dark blue line). The dashed line shows the climatology obtained by averaging the temperatures for each date over the years 1958–2002 using ERA-40 data (the land–sea mask differs very slightly from the operational one).

Atmospheric flow anomalies in the Northern Hemisphere

Figure 2 shows monthly anomalies of low-level (850 mbar) streamfunction* for May to August 2003. European weather was dominated by anomalous anticyclonic conditions (high values of streamfunction) throughout the period, beginning in May with a marked northward displacement of the subtropical Azores anticyclone, extending from the mid-Atlantic through to eastern Europe, and a general strengthening of westerly flow on its poleward flank over the UK and southern Scandinavia. For each of the subsequent summer months, a pattern of anomalies persisted over the Atlantic sector, comprising low (cyclonic) streamfunction values over the northern coast of South America, high (anticyclonic) values north-east of the Caribbean, low values in the central or north-east Atlantic and high values over continental Europe. During May, June and August there was also an obvious train of anomalies (low–high–low streamfunction) extending across Russia to the Pacific coast. This pattern is also seen along 45°N during July, although a much stronger anticyclonic anomaly extended across Scandinavia to the Urals. The European anomaly varied through the summer, being stronger and with more anticyclonic curvature in June and August, and weaker in July. The cyclonic anomaly over the Atlantic was situated west of the UK in June and July and further south-

*Streamfunction plotted on pressure levels indicates the direction and strength of the wind (more precisely its rotational component) – wind arrows point along streamfunction contours (clockwise around positive centres) and its gradient indicates wind strength. Anomalies are calculated by removing the climatological monthly means.

west in August. Throughout the 4-month period, the anomalous flow over the UK contained a southerly component, but it gradually turned from being south-westerly with cyclonic curvature in May to being south-easterly with anticyclonic curvature in August. This indicates an increasing tendency to advect air at low levels over the UK from continental Europe rather than from the Atlantic.

The large-scale anomalies at mid-tropospheric levels (Grazzini *et al.* 2003) were very similar to those just described at low levels, indicating an approximately equivalent barotropic vertical structure in the monthly averages. The streamfunction anomalies of alternating sign from South America to Europe and beyond suggest a Rossby-wave signal propagating from tropical America.

Influence of flow anomalies on radiative fluxes and sea surface temperature

The observed top-of-atmosphere (TOA) outgoing long-wave radiation (OLR) anomalies for June–August 2003 (Fig. 3) show increased OLR over Europe, associated with reduced cloud and precipitation (NOAA 2003) in the region of the anticyclonic anomaly. Over the North Atlantic, the OLR anomalies show a pattern with five zonal bands. Looking northwards from the equator, there was a high–low dipole straddling the climatological latitude (8–9°N) of the west African Intertropical Convergence Zone (ITCZ). This resulted from a northward shift and regional intensification of the ITCZ – throughout the rest of the tropics, apart from the north-west Indian Ocean, the ITCZ was weaker than normal (not shown here). The next band (anomalously high OLR) is associated with an intensification of the Azores anticyclone. At the same time, the Icelandic low was further south than normal, associated with enhanced cyclonic activity south of Iceland and reduced cyclonic activity to the north of 60°N. The TOA net radiative fluxes from ECMWF 0–24 hour forecasts (not shown) also possess the same banded pattern, with anomalously large downward fluxes in the strip stretching across the Atlantic west-south-west of Portugal and reduced fluxes to the north and south. The same pattern is also seen in the net radiative fluxes at the surface but with reduced amplitude. Taken together the fluxes are indicative over the North Atlantic of reduced cloud to the west-south-west of Portugal and increased cloud to the south and north of this strip, which are associated with intensification of the Azores anticyclone, a northward shift in the ITCZ and a southward shift in the summer extratropical storm track (seen in Fig. 2 as a low streamfunction anomaly which was west of Ireland in June and July).

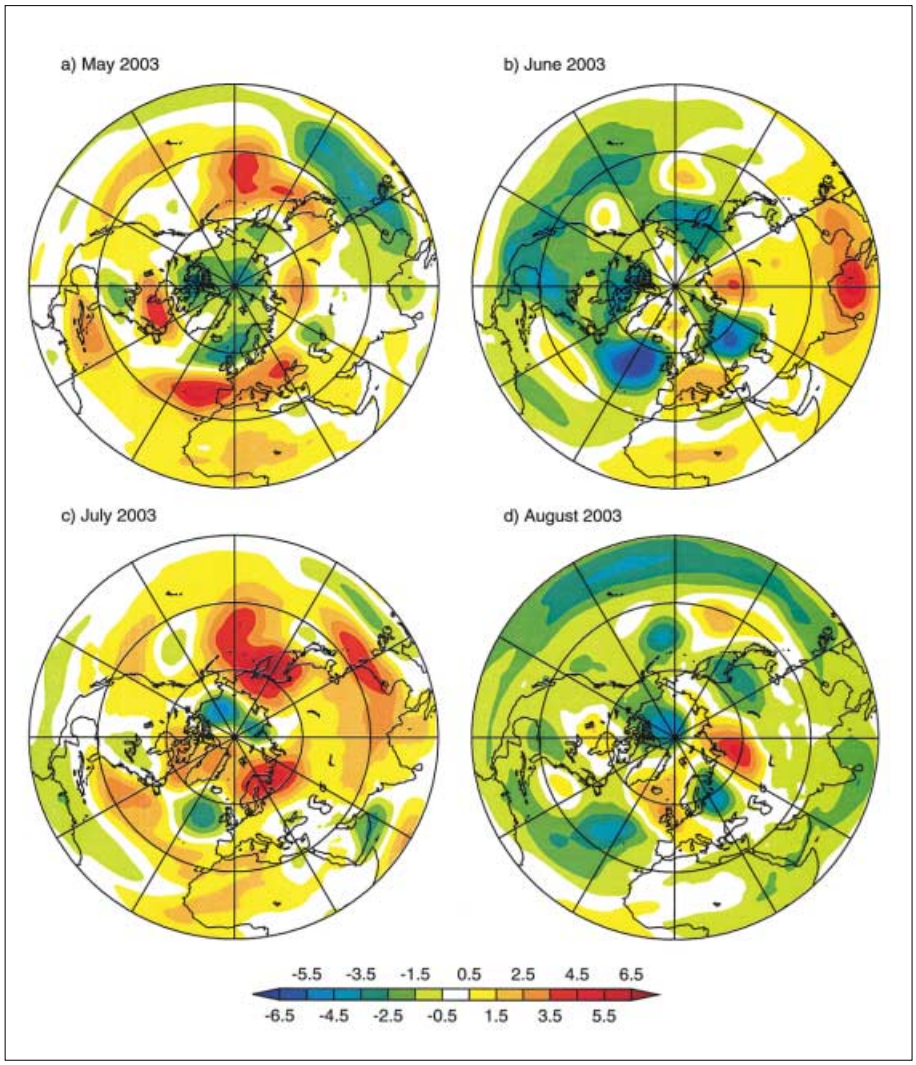

Fig. 2 Monthly anomalies of streamfunction on the 850 mbar pressure level for May–August 2003. The anomalies are deviations of the ECMWF operational analyses for 2003 from the ERA-40 climatology for 1958–2002. Shading interval 10^6 $m^2 s^{-1}$.

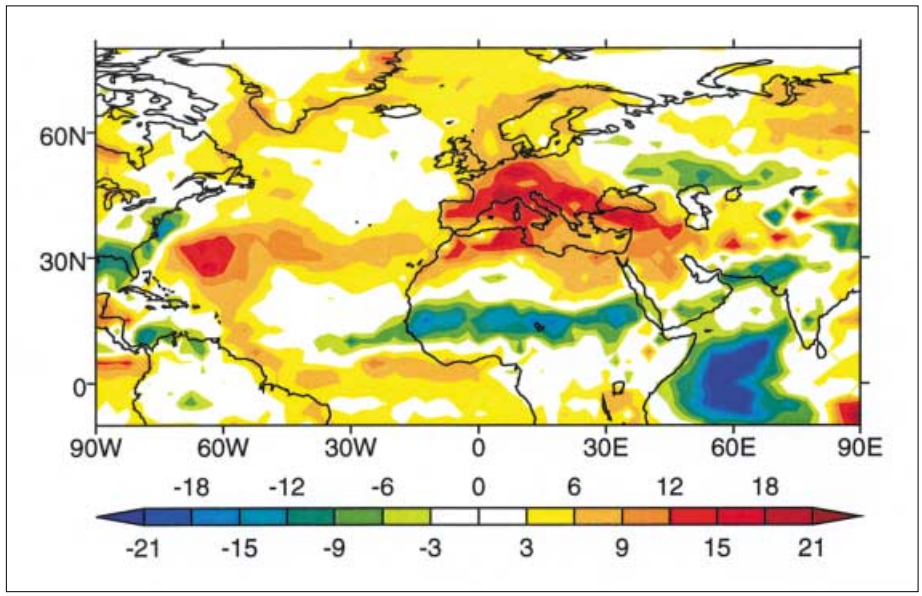

Fig. 3 NOAA satellite-observed outgoing long-wave radiation anomalies averaged over June–August 2003, calculated as departures from the 1979–95 climatological average. Units are W m^{-2}.

Figure 4 shows the evolution of sea surface temperature (SST) anomalies between May and August. At the end of April and in early May, the Mediterranean warmed rapidly (the SST anomalies were less than 0.5 degC on average during April). In the east Atlantic a banded pattern emerged with five distinct centres: anomalously high SST to the south of the ITCZ; low on its northern flank; high SST to the west-south-west of Portugal; low SST between Ireland and Newfoundland; and high SST poleward of 60°N. In June, both the warmth of the Mediterranean and the pattern in the east Atlantic intensified. During July, the unusually high Mediterranean SST persisted with record-breaking temperatures exceeding 30 °C (Grazzini *et al.* 2003), while the air temperature over Europe was less anomalous. In the Atlantic the high SST to the west-south-west of Portugal and the low SST to the west of Ireland further intensified and the high SSTs off the Norwegian coast became especially strong under the clear skies associated with the anticylonic anomaly centred over Scandinavia (Fig. 2). The Atlantic banded pattern in radiative fluxes was particularly strong in May but weak in July. In contrast, the SST pattern amplified most rapidly between May and June and hardly changed between July and August, suggesting that the SST anomalies responded passively to the radiative flux anomalies.

Globally, the strongest OLR anomaly (less than –30 W m^{-2}) during this period was situated above anomalously high SST in the north-west Indian Ocean. This SST anomaly (Fig. 4) was located off the coast of Somalia in May, moving north to the Arabian Sea by July. It was strongest in June (more than 1.5 degC) and may have been associated with the late onset of the Asian summer monsoon in 2003, a weaker Somali jet in the lower troposphere along the east African coast, and weaker upwelling of cold water. Rodwell and Hoskins (1996) have demonstrated that the atmospheric response to heating in the monsoon region includes enhanced descent over the eastern Mediterranean. This strong descent keeps the air above the Mediterranean particularly dry and suppresses convection, resulting in the hot, dry Mediterranean summer climate. However, the late monsoon onset in 2003 cannot account for the exceptionally hot, dry conditions over Europe in May and June. Possible teleconnections relating the European summer to anomalies further afield include the overall intensification of the Azores high and northward shift of the west African ITCZ, and the Rossby-wave signal from tropical America.

Steady anticyclone and descending air over western Europe

The most extreme temperatures in western Europe were experienced from 6 to 12 August. During this period there were very slack gradients in mean sea-level pressure but there was a weak signature of blocking, with a high over the UK and North Sea, a low over Iberia, and a high over the western Mediterranean (see *Weather Log* – corrected maps for August 2003 were distributed with the November issue of *Weather*). The blocking system was centred over northern France. Figure 5 shows 7-day trajectories calculated backwards in time using the UGAMP trajectory model (Methven 1997) from a point 500 m above Paris every 6 hours during this period. The steadiness of the anticyclone had the result that air was trapped within it and travelled a very short distance (compared with typical trajectories for the European sector) during the week preceding arrival. While caught in the anticyclone, the trajectories generally descended.

Above the top of the daytime boundary layer, airmasses experienced cooling at a steady rate, as seen by the change in potential temperature following trajectories

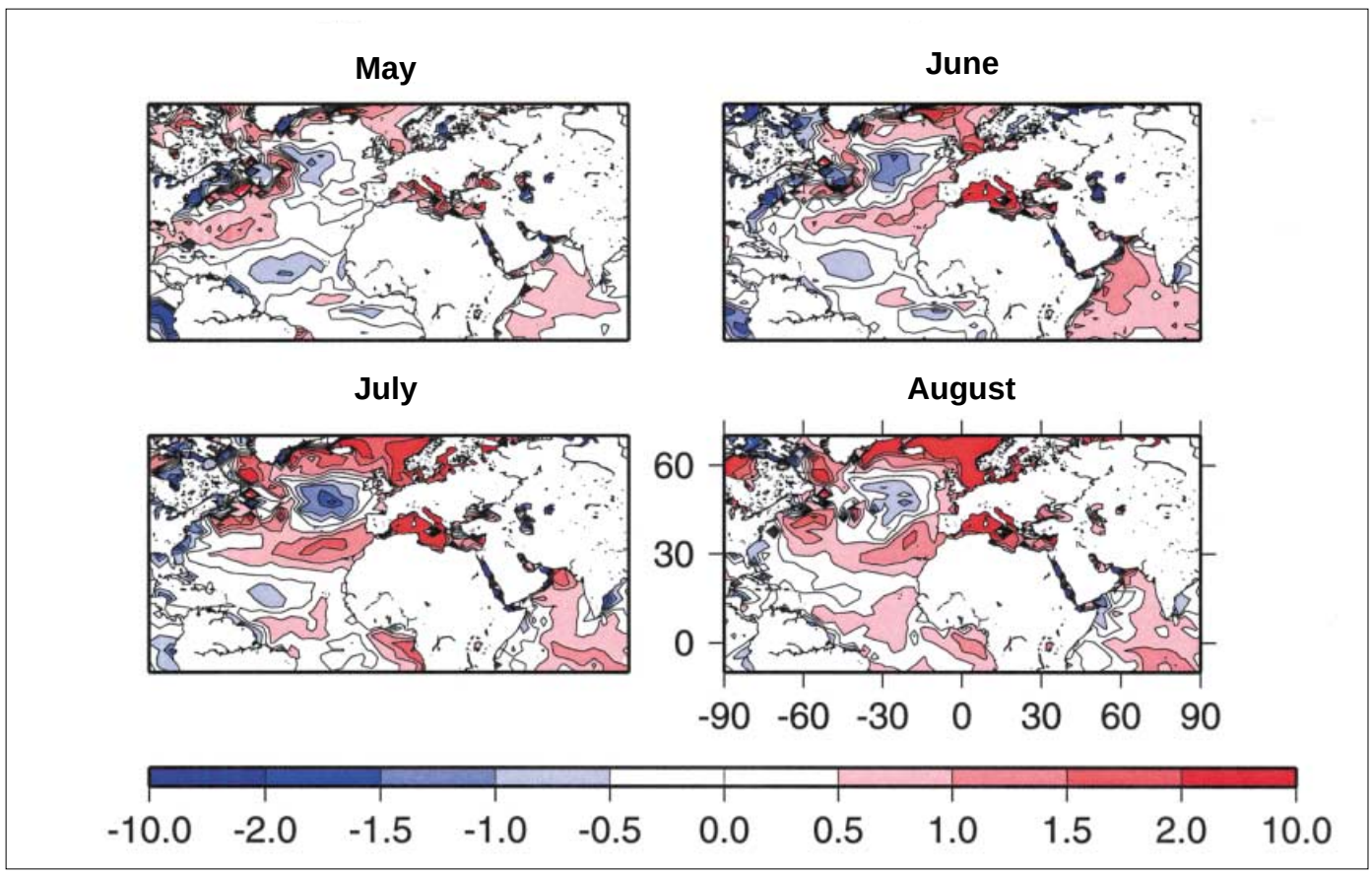

Fig. 4 Monthly mean SST anomalies (skin temperature, degC) for May–August 2003. The anomalies are calculated as the deviation of ECMWF operational analyses from the ERA-40 climatology for 1958–2001.

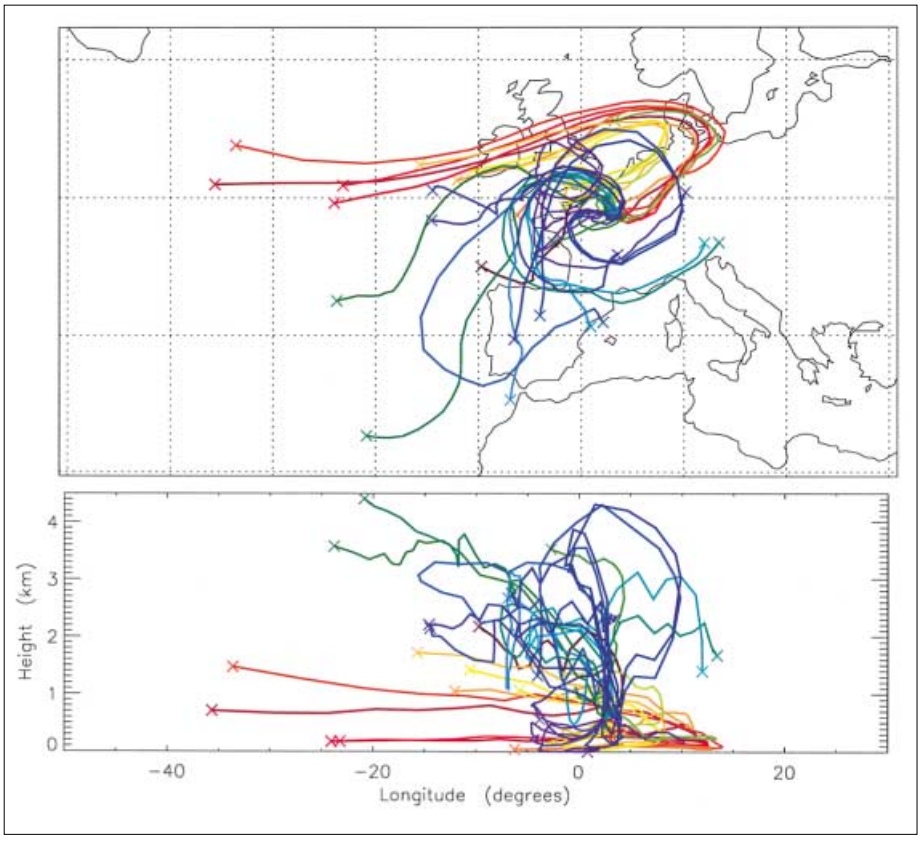

Fig. 5 Trajectories calculated following the winds from ECMWF analyses backwards in time for 7 days from 500 m above Paris, releasing one every 6 hours for 6–12 August 2003. The bottom panel plots the longitude–height coordinates of each trajectory. The colours correspond to the 'arrival time' above Paris passing from red to yellow to green to blue.

(Fig. 6(a)) that arrived at 1800 GMT on 12 August (the hottest day in Paris, with temperature reaching 40.0 °C). Potential temperature takes account of adiabatic compression of unsaturated air parcels so that its value would be constant along 3D trajectories in the absence of heat exchange; the calculation is sufficiently accurate that changes greater than 1 K can be related to diabatic heating or cooling (Methven *et al.* 2003). The potential temperature decrease is indicative of radiative cooling to space in the clear air within the anticyclone (at a rate of about -2 K day^{-1}). The cooling enabled steady descent across surfaces of constant potential temperature in the stably stratified free troposphere. Note that the two trajectories that arrived at the top of the profile had experienced strong heating between 10 and 6 days earlier. This did not occur over Europe but within a warm conveyor belt – a body of air that condensed water vapour and released latent heat as it ascended following the US east coast to Newfoundland. The remaining trajectories circled anticyclonically around Europe.

During the heatwave the surface was heated strongly, and turbulence and dry convection (*i.e.* without condensation) enabled the boundary layer to extend much higher than normal. The red curves in Fig. 6(b) show profiles at 1800 GMT above Paris derived from ECMWF analyses – virtual potential temperature* was mixed throughout the boundary layer from the ground up to about 4 km by late afternoon, resulting in an almost adiabatic (convectively neutral) profile. The atmosphere was only out of direct contact with the ground above 4 km or for potential temperatures greater than 313 K. It is clear from Fig. 6(a) that radiative cooling occurred above 313 K but that potential temperature remained fairly constant following trajectories in the adiabatic layer, presumably because turbulent mixing from the hot surface overcame the cooling. At night the surface cooled rapidly, resulting in a very stable nocturnal boundary layer up to about 500 m as seen in the 0600 GMT profiles (black curves in Fig. 6(b)). Above this the residual adiabatic layer remained. The red–orange trajectories in Fig. 6(a) stay below 500 m and therefore show the strong diurnal variation within the boundary layer associated with the surface heat budget and gradual warming as the hottest day approached.

Given the extreme surface temperatures and high relative humidity in the boundary layer in the morning (not shown), it is perhaps surprising that moist convection, associated with condensation in ascending air and cloud formation, was not widespread during this period. However, the strong radiative cooling and descent would tend to suppress convection, thus maintaining clear-sky conditions.

Heat budget for the atmosphere above Europe

Since the flow was almost stagnant, hot air was not brought into Europe from further afield. The regional heat budget must have enabled the extremely high temperatures to occur.

The impact of the anomalous anticyclonic flow and clear-sky conditions is evident in estimates of the components of the TOA and surface energy budget over continental Europe. We have used data for 2003 from short-term (0–24 hour) forecasts of the operational ECMWF model, and anomalies have been computed relative to the equivalent ERA-40 climatological data for the period 1958–2002. These are model products rather than directly analysed data, and they could be contaminated by any model spin-up* in the 0–24 hour forecast period and by any differences between the ERA-40 version of the model and the version that was operational in summer 2003. It is difficult to estimate the size of such errors, but the data have the advantage of being spatially comprehensive and consistent with the initial evolution of the ECMWF model forecasts, which are strongly constrained by the analysed initial state.

Monthly anomalies of the energy budget averaged over European land areas within the domain 0–20°E, 42.5–52.5°N (shaded in Fig. 1) are shown in Fig. 7. In each of the four months there was a positive (downward) net radiative flux anomaly at the TOA (red bars), tending to heat the land and atmospheric column, which ranged from approximately 10 W m^{-2} in May to 20 W m^{-2} in June.† The short-wave and long-wave components of this signal (not shown) are consistent with

*Potential temperature is the temperature that an air parcel would attain if moved adiabatically to a reference pressure (1000 mbar). Virtual potential temperature also takes account of the greater buoyancy of a moist parcel compared with surrounding dry air because water has a lower molecular weight than the average for dry air – whenever virtual potential temperature decreases with height the atmospheric column is convectively unstable.

*Model spin-up refers to any systematic adjustment with forecast time due to the initial data not being precisely consistent with the physical processes in a numerical weather prediction model.

†An unbalanced TOA flux anomaly of 10 W m^{-2} is equivalent to a heating rate of 2.5 K month^{-1} in either the entire atmospheric column or in 2.5 m of an ocean surface layer.

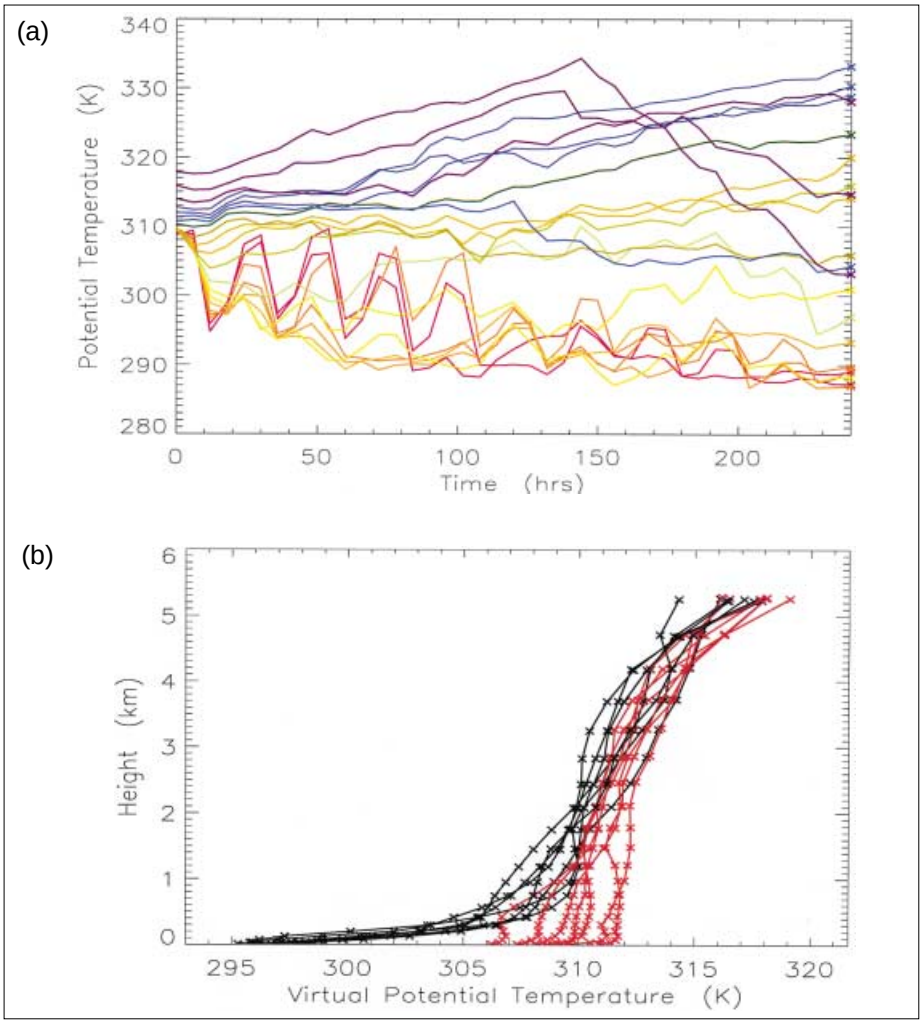

Fig. 6 (a) Potential temperature following trajectories backwards in time for 10 days (from left to right on the graph). The trajectories start at 1800 GMT on 12 August 2003 (going back to 2 August) from levels between the ground and 5 km above Paris. (b) Virtual potential temperature from the ECMWF analyses versus height for 6–12 August 2003. Red curves are for 1800 GMT, black curves for 0600 GMT on each day.

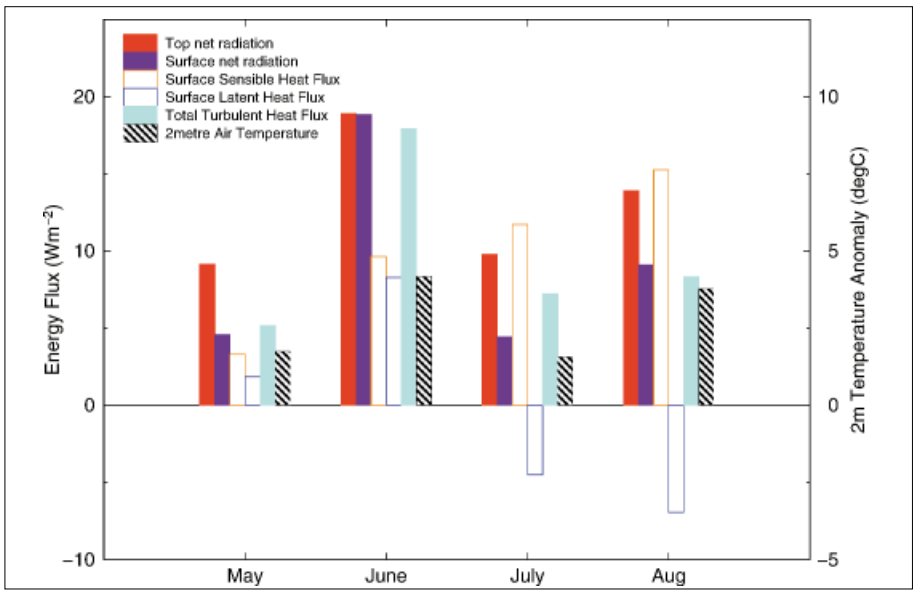

Fig. 7 Monthly anomalies in the energy budget for the European land area 0–20°E, 42.5–52.5°N, for May–August 2003. The bars correspond to anomalies in: TOA net radiative flux (red), surface net radiative flux (purple), surface sensible heat flux (open, orange), surface latent heat flux (open, blue) and surface turbulent flux (sensible heat flux + latent heat flux) (blue). Data are from ECMWF short-term forecasts (0–24 hours), computed as departures from the ERA-40 climatology for 1958–2002. Downward radiative fluxes and upward turbulent fluxes are positive. Monthly anomalies in 2 m temperature are also shown (hatched).

reduced cloud cover, namely a positive OLR anomaly in each month which was more than compensated by a reduction in reflected short-wave radiation. Figure 7 implies that less than half of this anomalous radiative forcing was used to heat the atmospheric column, so that more than half was available at the land surface (purple bars). On a monthly time-scale, the increased surface radiative forcing was approximately balanced by increased (upward) turbulent fluxes (blue bars). The flux anomalies in June were remarkable, with almost the entire 20 W m^{-2} TOA forcing anomaly available at the surface and balanced by the turbulent flux anomaly. Notably, the seasonal evolution of the sensible and latent heat flux components was quite different; the latent heat flux anomaly was initially positive but became increasingly negative, indicative of a gradual drying of the land surface through the summer, whereas the sensible heat flux anomaly remained positive and increased, associated with increasing surface temperatures. Moreover, the energy budget clearly shows that the negative latent heat flux anomalies associated with soil drying acted to amplify the radiative forcing of surface air temperature in July and August, doubling the (relatively weak) 4 W m^{-2} radiative anomaly in July and increasing the stronger August anomaly by almost 80%.

Detailed observations of the surface energy budget at Reading

The ECMWF model indicates the importance of the land surface in the gradual development of higher air temperatures over Europe. This process is further investigated by analysing measurements of temperature, humidity and surface energy fluxes which were obtained during August 2003 using automated instruments* at the Department of Meteorology's field site (situated on the University of Reading's Whiteknights campus).

Two platinum resistance thermometer sensors to BS1904 (Class A), were housed in a Casella double-louvred small Stevenson screen, with one temperature sensor being operated as a wet bulb. The resistance changes were converted to voltages using a stable linearised Wheatstone bridge circuit (Harrison and Pedder 2001). Both temperature sensors had previously been individually calibrated in a water bath, using an ASL F25 platinum resistance thermometer traceable to national standards. Global and diffuse solar irradiances, S_g and S_d, were measured using two Kipp and Zonen CM5 solarimeters. The net radiative flux, R_n, and ground heat flux, G, were determined using a Kipp and Zonen NR-LITE radiometer and a

*http://www.met.rdg.ac.uk/~fsdata/metsite.html.

Table 1

Manual observations, taken at 0900 GMT in August 2003, from the University of Reading field site of daily maximum and minimum temperatures, and sunshine hours from a Campbell–Stokes instrument

Date in Aug.	Day number	Max. temp. (°C)	Min. temp. (°C)	Sunshine duration (hours)
3rd	215	28.1	10.4	13.4
4th	216	31.2	13.2	11.2
5th	217	31.9	18.4	9.4
6th	218	32.9	18.1	13.0
7th	219	29.2	16.5	10.0
8th	220	29.8	16.1	12.4
9th	221	34.2	16.4	12.7
10th	222	36.4	16.2	11.6
11th	223	33.3	19.9	10.8
12th	224	28.7	18.0	6.3
13th	225	27.7	15.6	11.1

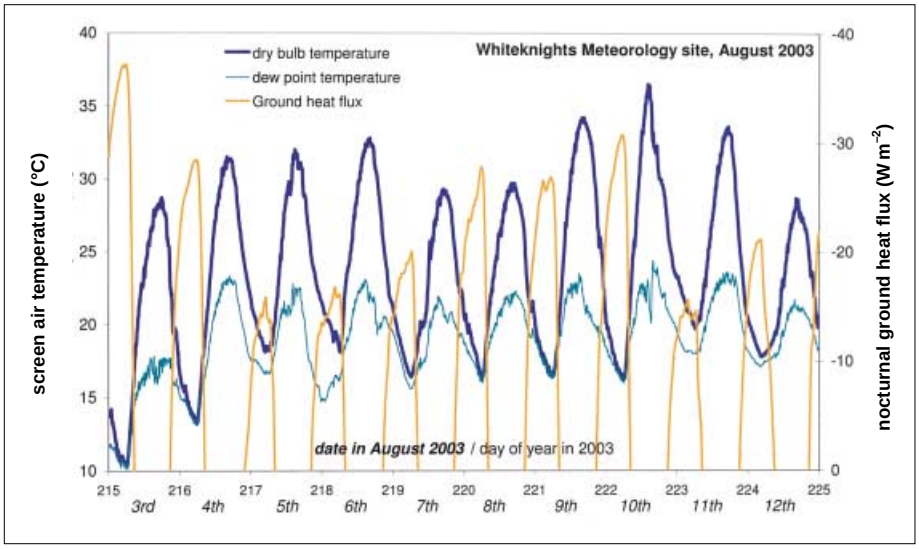

Fig. 8 Time-series of automatic temperature measurements obtained at the University of Reading during early August 2003. Nocturnal ground heat flux (negative values represent heat leaving the soil) is also shown.

McVan HP3 sensor respectively. For S_g, S_d, R_n and G, high-gain thermally stable amplifiers were used to amplify the microvolt sensor signals to high-level signals for a 12-bit analogue to digital converter. The high-level signals were recorded as 5-minute averages derived from 1 Hz samples, as described by Aplin and Harrison (2003).

As well as automatic readings, manual observations are taken at 0900 GMT at Reading from thermometers in a large Stevenson screen. Table 1 shows a summary of the observations obtained during August 2003. The maximum temperature of 36.4 °C on Sunday 10 August was the highest temperature since the record began on 1 January 1968. Two of the four daily maximum temperatures of 34.0 °C or more occurring since the beginning of the Reading records were in August 2003; the others were on 26 June 1976 (34.0 °C) and 3 August 1990 (35.5 °C).

Figure 8 shows the Reading temperature time-series for 3–12 August 2003. For 7–10 August, there was a rapid rise in the maximum temperatures, which generally occurred in the mid or late afternoons. The minimum nocturnal temperatures for each of the preceding nights were relatively constant, with the air cooling briefly to its dew point of that time. On 10 August, the maximum temperature was reached earlier (at 1410 GMT) than on the previous three days, following a more rapid rise in temperature during the morning. The actual diurnal variation for 10 August 2003 is given in Fig. 9, which shows the 5-minute average values of air temperature, diffuse and global solar irradiances, the net radiation and ground heat fluxes. A small amount of cloud between 1430 and 1545 GMT, associated with a cloud-band marked as an upper-level trough ahead of a cold front in the Met Office surface analysis (as discussed in Burt, this issue), probably prevented a higher maximum temperature from occurring.

The nocturnal ground heat flux (G) is also shown in Fig. 8. It is clear that $-G$ (which is a measure of heat leaving the soil) increased steadily from 5 to 10 August, although there was no associated change in minimum air temperature. Note that during the night preceding the hottest day (10 August), G became more negative until, by dawn, it balanced the net radiation which was almost steady throughout the night (Fig. 9). The increasing cancellation of radiative cooling by the ground heat flux slowed the nocturnal decrease in surface air temperature. Interestingly, although the period was dry in the sense that relative humidity was low during the day and precipitation did not occur, the air held sufficient moisture to saturate near the ground during the coldest hours of the night. Dew point was reached a few hours before dawn and the latent heat released by condensation would also slow the temperature fall. The nocturnal ground heat flux would have had a more significant impact in maintaining a higher minimum air temperature because the nocturnal boundary layer was shallow (evident for Paris in Fig. 6(b)). For example, an upward ground heat flux of 10 W m^{-2} would heat a 100 m atmospheric layer at around 0.3 K hour^{-1}. The maximum in the nocturnal heat flux (just over 30 W m^{-2}) was in the early hours of 10 August (day 222). The heat leaving the dry soil also contributed to the rather rapid rise in temperature during the morning.

Conclusions

The extreme temperatures and lack of precipitation in Europe from May to August 2003 were related to persistent anticyclonic conditions throughout the period. Over the east Atlantic, during May the Azores anticyclone and west African ITCZ were both displaced to the north, while the extratropical storm track was concentrated further south than normal, resulting in a pattern with five zonal bands in cloud and radiative forcing anomalies both at the surface and at TOA. The anomalously clear skies and downward net radiative fluxes led to high SSTs in a strip extending to the west-south-west of Portugal (with flanking low SST anomalies to the north and south). They also contributed to a strong loss of moisture from the European land surface. During June, the storm track shifted even further south and the anomalous high was much weaker over the Atlantic. However, the high persisted over Europe, resulting in extremely strong radiative anomalies, heating of the land surface, and enhanced latent and sensible heat fluxes into the atmosphere which together almost balanced the radiative anomalies. The land surface over central Europe warmed and dried to such an extent that, during July, when the radiative forcing was weaker, the latent heat fluxes were anomalously negative, due to lack of soil moisture, and the sensible heat fluxes were higher

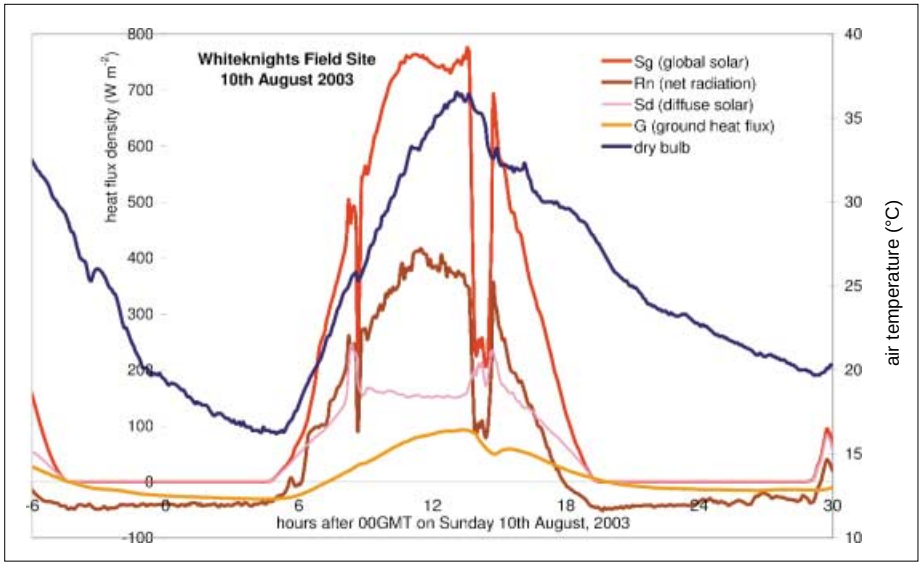

Fig. 9 Surface solar irradiances, net radiation and ground heat fluxes measured at the University of Reading during 10 August 2003. Simultaneous measurements of screen air temperature are also shown.

than usual due to the higher surface temperatures. During June and July, extratropical cyclones tracked further south than average towards Ireland before deflecting polewards around the anticyclonic ridge over central Europe. Consequently, the west coast of Europe received more precipitation than average in these months (Fig. 1 of Fink *et al.*, this issue). However, in the eastern UK the higher than average temperatures must have resulted in higher evaporation, maintaining dry land surface conditions. In August a blocking regime resumed over the whole of Europe, the absence of clouds again enhanced the radiative forcing, and the temperature increase at the surface was exacerbated by the inability of latent heat fluxes to transfer heat upwards due to the lack of moisture availability. Surface heat balance was almost achieved by the increase in sensible heat fluxes from the extremely hot land surface.

Observations taken at the University of Reading indicate that the ground played an important role in the accumulation of heat during the day and its gradual release at night. This acted to offset night-time cooling driven by upward long-wave radiation under clear skies, slowing the decrease in air temperature before sunrise. The impact on surface air temperature was more significant because the nocturnal boundary layer was very shallow in anticyclonic conditions. Therefore, the strong ground heat flux contributed to exceptionally warm nights, sustaining the thermal stress which led to the increased human mortality across Europe (WHO 2003).

At Reading the record-breaking temperature on 10 August could have been higher had cloud not passed over the area at about 1430 GMT. Examination of satellite images (see, for example, the image shown on the front cover) reveals that this cloud was part of a band ahead of a weak cold front which progressed very slowly across England during 11 and 12 August towards France. The highest temperature in Paris was recorded on 12 August and the temperatures fell by 6 degC the next day, heralding the end of one of the most severe heatwaves ever experienced in Europe.

In summer 2003 the large-scale atmospheric circulation enabled a dominance of the local heat balance over Europe under clear skies and with an increasingly dry land surface – the result was the exceptionally high temperatures. It is not known at this time why the large-scale circulation had the character it did.

Acknowledgements

Interpolated OLR data used in Fig. 3 were provided by the NOAA-CIRES Climate Diagnostics Center, Boulder, Colorado, USA, from their website at http://www.cdc.noaa.gov/. John Methven is grateful for an Advanced Fellowship sponsored jointly by the Natural Environment Research Council and the Environment Agency.

References

Aplin, K. L. and Harrison, R. G. (2003) Meteorological effects of the eclipse of 11th August 1999 in cloudy and clear conditions. *Proc. R. Soc. London A*, **459,** pp. 353–372, doi: 10.1098/rspa.2002.1042

Beniston, M. (2004) The 2003 heat wave in Europe: A shape of things to come? An analysis based on Swiss climatological data and model simulations. *Geophys. Res. Lett.*, **31,** pp. 2022–2026, L02202, doi:10.1029/2003GL018857

Grazzini, F., Ferranti, L., Lalaurette, F. and Vitard, F. (2003) The exceptional warm anomalies of summer 2003. *ECMWF Newsletter*, **99,** pp. 2–8

Harrison, R. G. and Pedder, M. A. (2001) Fine wire thermometer for air temperature measurement. *Rev. Sci. Inst.*, **72,** pp. 1539–1541

Kovats, S., Wolf, T. and Menne, B. (2004) Heatwave of August 2003 in Europe: provisional estimates of the impact on mortality. *Eurosurveillance Weekly*, **8,** 11 March 2004, available online from http://www.eurosurveillance.org/ew/2004/040311.asp#7

Methven, J. (1997) *Offline trajectories: Calculation and accuracy*. Technical Report 44, UK Universities Global Atmospheric Modelling Programme, Department of Meteorology, University of Reading

Methven, J., Arnold, S. R., O'Connor, F. M., Barjat, H., Dewey, K., Kent, J. and Brough, N. (2003) Estimating photochemically produced ozone throughout a domain using flight data and a Lagrangian model. *J. Geophys. Res.*, **108,** 4271, doi:10.1029/2002JD002955

NOAA (2003) *Climate Diagnostics Bulletin* Nos. 03/6–8. Available from Climate Prediction Center, Camp Springs, Maryland, USA, http://www.cpc.ncep.noaa.gov/products/analysis_monitoring/CDB_archive.html

Rodwell, M. J. and Hoskins, B. J. (1996) Monsoons and the dynamics of deserts. *Q. J. R. Meteorol. Soc.*, **122,** pp. 1385–1404

Schär, C., Vidale, P. L., Lüthi, D., Frei, C., Häberli, C., Liniger, M. A. and Appenzeller, C. (2004) The role of increasing temperature variability in European summer heatwaves. *Nature*, **427,** pp. 332–336

Simmons, A. J. and Gibson, J. K. (2000) *The ERA-40 Project Plan.* ERA-40 Project Report Series No. 1, ECMWF, Reading, UK

WHO (2003) *Health effects of extreme weather events: WHO's early findings to be presented at the World Climate Change Conference.* Available online from http://www.euro.who.int/mediacentre/PR/2003/20030929_1

Correspondence to: Dr J. Methven, Department of Meteorology, University of Reading, PO Box 243, Reading RG6 6BB.
e-mail: swrmethn@met.reading.ac.uk

doi: 10.1256/wea.74.04